Piezofibre composite transducers for next generation 3D USCT

M. Zapf[1], K. Hohlfeld[2], P. Pfistner[1], C. Imbracio Liberman[1], K.W.A. van Dongen[4], H. Gemmeke[1], N.V. Ruiter[1], A. Michaelis[2,3], S. Gebhardt[3]

[1] *1Karlsruhe Institute of Technology, Institute for Data Processing and Electronics, Karlsruhe, Germany*
E-mail: michael.zapf@kit.edu
[2] *Institute of Materials Science, TU Dresden, Dresden, Germany*
[3] *IKTS, Fraunhofer Institute for Ceramic Technologies and Systems, Dresden, Germany*
[4] *Department of Imaging Physics, Faculty of Applied Sciences, Delft University of Technology, Delft, the Netherlands*

Abstract

At the Karlsruhe Institue of Technology (KIT), a 3D-Ultrasound Computer Tomography (3D-USCT) medical imaging system for early breast cancer detection is currently developed. With the next generation of 3D-USCT 2.5, the current region of interest (ROI) of 10 x 10 x 10 cm³ shall be increased to 20 x 20 x 20 cm³ to allow reliable imaging results also for bigger female breasts. Therefore, the opening angle (OA) of the future transducers should be increased to approx. 60 ° at 3 dB while other characteristics such as bandwidth (BW) and resonance frequency should be preserved or even improved. Based on Fraunhofer IKTS Piezofibre composites utilized for transducer production, an optimization is performed on piezoelectric sensor geometry and size, type and structure of matching and backing layer and interconnection technology of the several parts of the transducer

Keywords: US transducer, composite materials, SAFT imaging, piezo fibre composite

1 Introduction

Breast cancer is the most common cancer in females in the world [1, 2].The spreading probability of the tumor and thus the chances of survival are correlated to its size [3]. Therefore, early detection plays a vital role in reducing the mortality of breast cancer.

KIT developed a 3D USCT imaging system for early breast cancer detection [4] [5] [6]. Imaging is achieved by Synthetic Aperture Focusing Technique (SAFT) using a multistatic setup of 2041 ultrasound transducers, grouped in 157 Transducer Array Systems (TAS) embedded in a semi-elliposoidal aperture (Figure 1). A center frequency of 2.5 MHz is applied. The bandwidth (BW) and opening angle (OA) at 3 dB amount to 1 MHz and 36°, respectively. The fundamental connection between an ultrasound transducer's emission and reception sensitivity in the azimuth and elevation angle space is the tranducer's aperture size.

Finite element (FE) simulations have shown that a reduction in size of the current generation transducer elements by roughly a factor 2 from 900 µm to 500 µm is required to realize an OA of 60 ° at 3 dB. Wave simulations also revealed that a circular instead of the current rectangular aperture will result in additional homogeneity of the sound field.

As circular sensors are difficult to produce in the dice-and-fill approach, octagon shaped transducers are built for USCT 2.5. The octagon shape can be achieved with the established dice-and-fill technique by adding 2 sawing cuts. Furthermore, inspired by compressive sensing, an irregular distribution of the sensor elements on the TAS is applied which covers almost the full surface area of US transducer. Further improvements are introduced regarding connectivity and bandwidth.

2 Motivation

2.1 3D USCT 2.0 current status

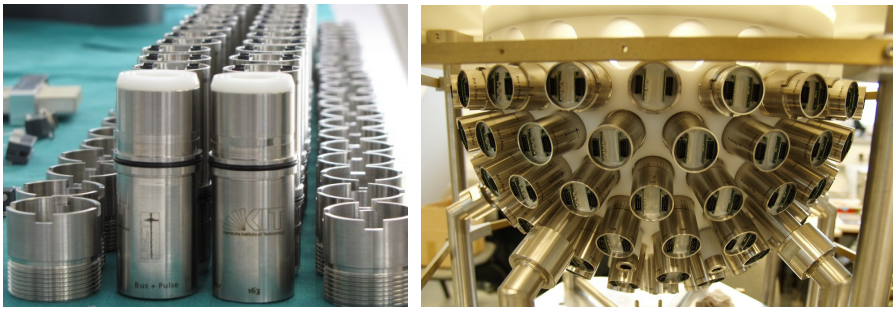

Figure 1: Left: USCT 2.0 TAS systems transducers before assembly in the final system. Right: Semi-ellipsoidal aperture of USCT 2.0

The current USCT 2.0 system covers a ROI of 10 x 10 x 10 cm^3. Results from the clinical trial with the University hospital Jena indicated that a bigger ROI is beneficial to cover a broader range of breasts and adapt also to the buoyance broadening effect of floating breasts [5]. Each of the 157 TAS consists of 13 rectangular transducer elements 0.9 x 0.9 mm in size

[7]. One TAS consists of four emitters, nine receivers which are regularly distributed in a square grid, covering just the inner part of the TAS (Figure 2).

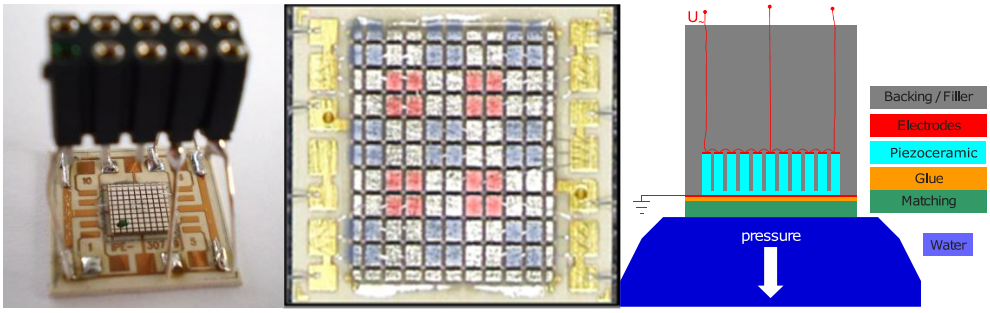

Figure 2: Left: Inner part of one TAS of USCT 2.0. Middle: Closer view on the piezoelectric elements. Four squares are connected to form one receiver (blue) or emitter (red). Right: Schematic side-view on one TAS of USCT 2.0.

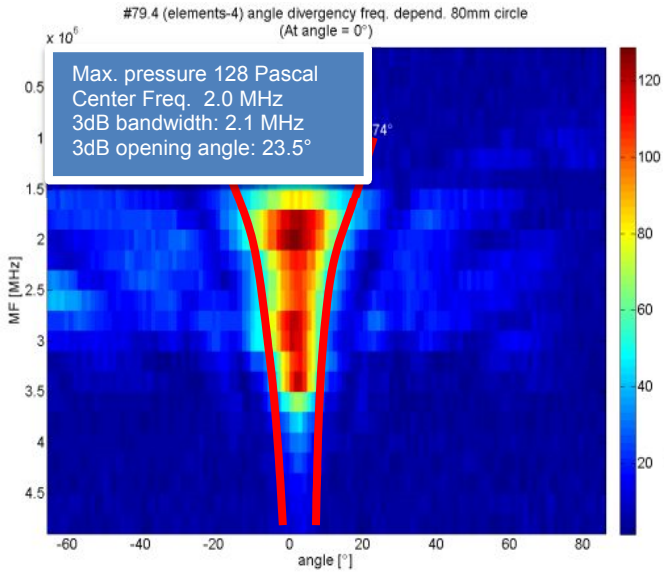

Figure 3: Frequency over angle for one element of one TAS of USCT 2.0. Given with red-lines approx. the frequency dependend 3dB opening angle.

2.2 Design considerations for next generation 3D USCT

For next generation 3D USCT (called 3D USCT 2.5) several should be improved contribute to a homogenous illumination and imaging contrast.

2.2.1 Opening angle (OA)

The benefit of an increased OA is schematically shown in Figure 4.

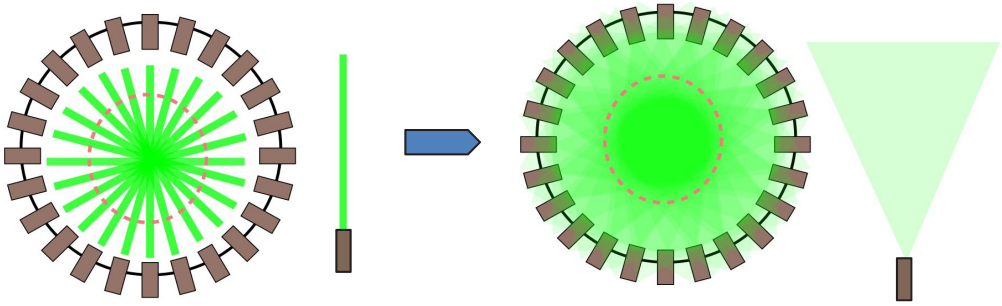

Figure 4: Illumination of an exemplary 3D-USCT system (top down view) for transducers with a small OA (left) compared to transducers with a larger OA (right).

2.2.2 Bandwidth

The BW of the transducers should be increased, as a larger BW better contrast in SAFT images, see Fig. 6. An increased coverage of the K-space, the spatial Fourier domain, can be achieved by broadening the bandwidth of the transducers. [8] Also, full wave inversion schemes and transmission tomography benefits from lower frequency components included in a broader bandwidth which covers also lower frequency down to 0.5 MHz.

2.2.3 Irregular distribution of sensor

An irregular distribution of the elements leads to greater coverage of the ROI and more homogeneous illumination. This is inspired by the "compressive sampling" concept now utilized in many apertures of various imaging systems as also ultra sound imaging systems.

2.2.4 Reduction in sparsity of sampling

An upgrade from 13 to 17 elements is performed. There are still nine receivers but the number of emitters has been doubled from four to eight emitters. Electronic constraints inhibit an upgrade to 9 emitters for symmetric emitter/receiver distribution. More emitters reduce the sparsity in imaging, leading to a more homogeneous coverage of the ROI. The final transducer distribution is shown in Figure 14.

2.3 Simulations

2.3.1 MATLAB

Ultrasound wavefield emission simulations for different surface geometries ("transducer apertures") have been performed as "piston model". As it is well known from antenna and

transducer design, there is a reciprocal relationship between the element / aperture size, and the directivity / opening angle of the sound beam. A reduction in transducer sidelength / diameter from 900 µm to 550 µm should lead to an increase in OA to 50°-60° at 3 dB.

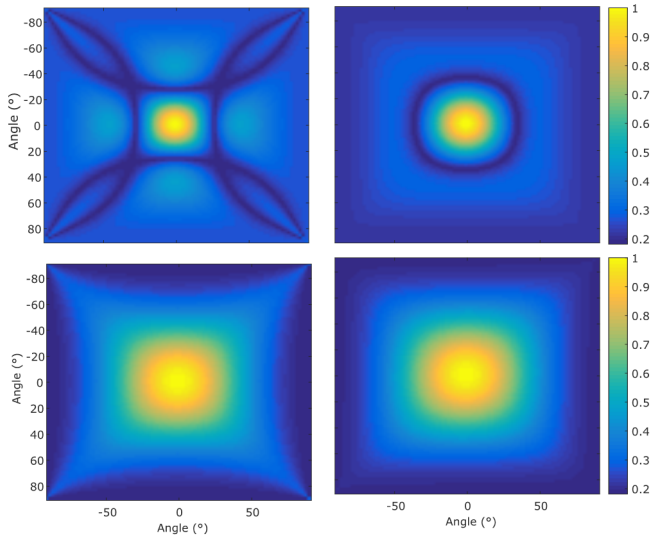

Figure 5: MATLAB aperture piston model simulations: US sound field for rectangular 0.9 mm (upper left), rectangular 0.4 mm (lower left), circular 0.94 mm (upper right) and circular 0.45 mm (lower right).

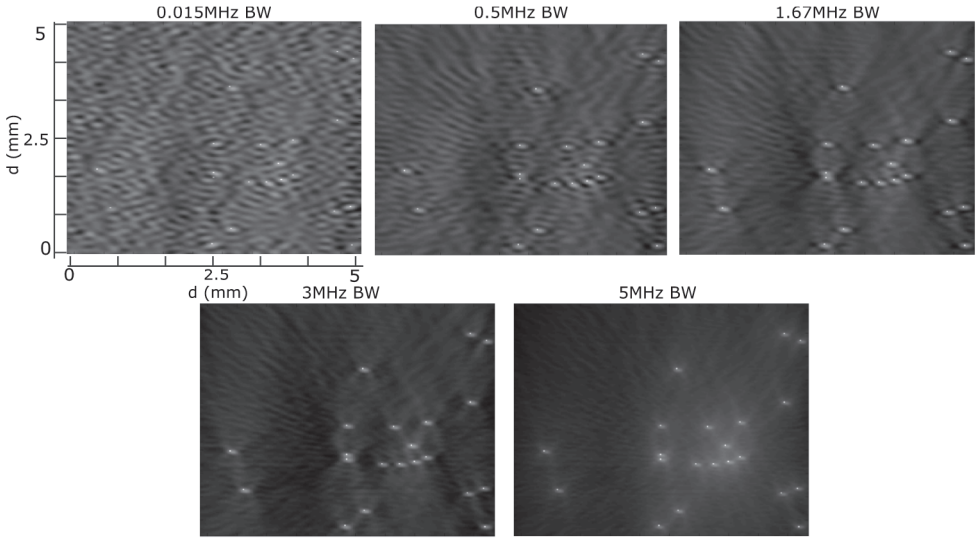

Figure 6: SAFT simulations for many point scatterers for varying BW. Contrast increases for broader bandwidth, while the resolution is more or less retained.

Circular elements express a more homogeneous sound over field compared to rectangular elements. (Figure 5).

SAFT simulations have been performed on point scatterers with varying BW (Figure 6). The results show that for SAFT image reconstruction, more BW leads to higher contrast in the images.

2.3.2 KLM

KLM simulations have been performed to find the ideal matching layer thickness for a broad BW. Simulations on TMM4 as a matching layer are shown in Figure 7. In the given configuration the resonance was the broadest for a 200 µm TMM4 layer due to two resonance peaks.

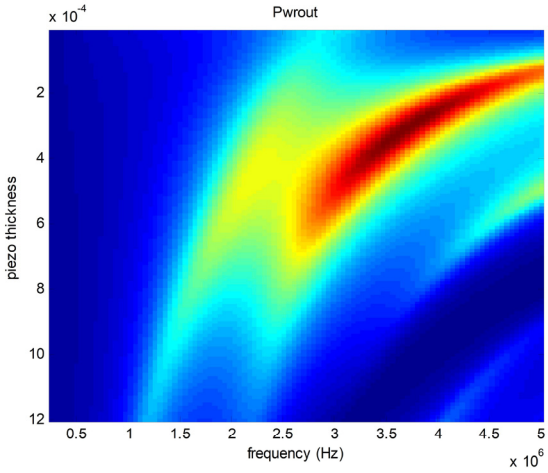

Figure 7: KLM model showing piezo thickness over frequency for a 200µm TMM4 matching layer with varying PZT thickness on the Y axis. X axis give the frequency range.

2.3.3 Finite element simulation

As 1D KLM simulations are insufficient to analyze lateral and shear wave effects of a design, a higher spatial dimensional simulation was utilized. Finite element (FE) simulations in 3D and 2D were performed. Also the impact of various materials on the Transducer performance were analyzed. PZflex was used as standard tool for piezoactive materials and non-piezoactive materials. The spatial properties of the transducer design was meshed with at least 3 times spatial sampling. Temporla sampling was derived automatically by the simulation tool, exported was the sound pressure field in each element in the water in the farfield in 2 to 6 cm distance.

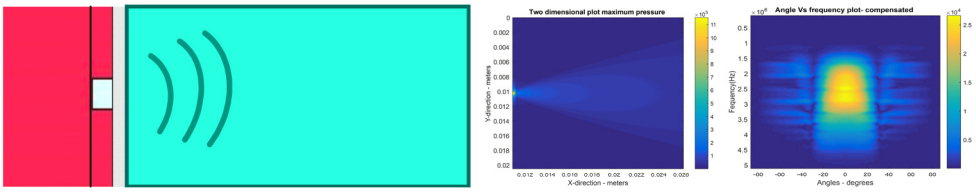

Figure 8: Left: Exemplary 2D PZFlex simulation model spanning 6cm in x and 2 cm in Y: Red: Backing + filling PU + Tungsten (12 MRayl): Red + bright blue: Piezofibrecompositedisc. (CeramTec Sonox 505 14.2 MRayl). Grey: Matching (TMM4 ca. 6.3 MRayl). Blue: Water (1.5 MRayl). Middle: Left: two-dimensional pressure plot X over Y, simulated by PZFlex for the setup described. Right: frequency over angle plot for the same setup.

3 Approach and method

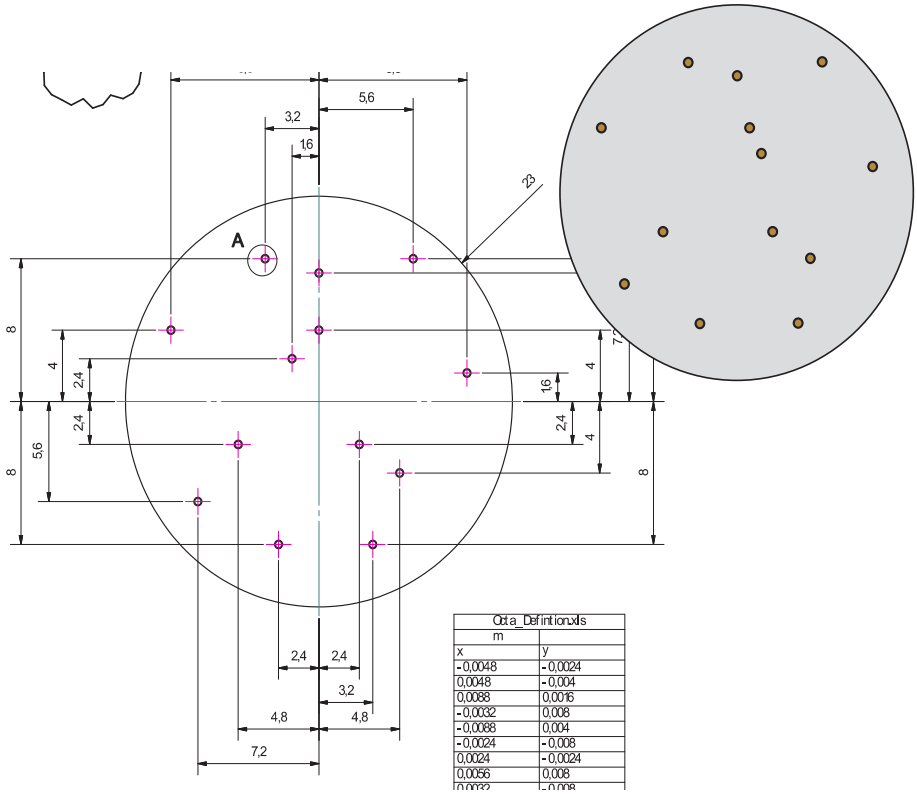

Figure 9: Definition of a pseudo random transducer distribution on the piezofibre disc. Original 13 element design (later extended to 17 elements).

The selected design is a pseudo-random distribution which should be homogenous distribution over the surface of the whole transducer array, while being irregular and non-periodic to minimize side lobes; this is inspired by compressive sampling techniques; see figure 9.

3.1 Piezofibre disc production

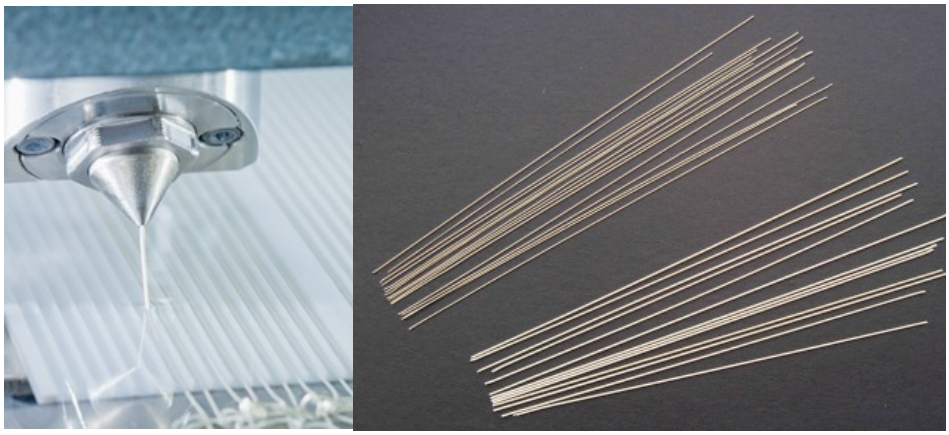

Figure 10: IKTS Piezofibre production process.

The FhG IKTS fiezofibre production process promises a cost reliable, reproducible and accurate build of arbitrary placed and sparse 2d transducer geometries. Additionally, a homogenous performance is to be expected due to production from a small number of fibres and piezo production batches.

The process starts from slicker with a liquid solvent which is pushed with a dispenser in a water bath and cures instantely in a green piezo fibre. These fibres are cured and hardened in a plumbum enriched atmosphere sinter oven [15,16].

The next steps is the placing of the pre-shrinked to ~470µm diameter fibres in metallic mask, see figure 4 top left. The mask with the piezo fibres is placed in a moulding container and filled with the epoxy substrate. The resulting block is milled to a round rod of approx. 14cm length and 2.3cm thickness. Two such rods are sufficient to satisfy the required 200 discs for an USCT. The rod is than sawed in discs of the desired thickness: for this analyzis 400, 550, 750, 1050, 1450, and 2050 µm thick discs were sawed with an in-hole saw.

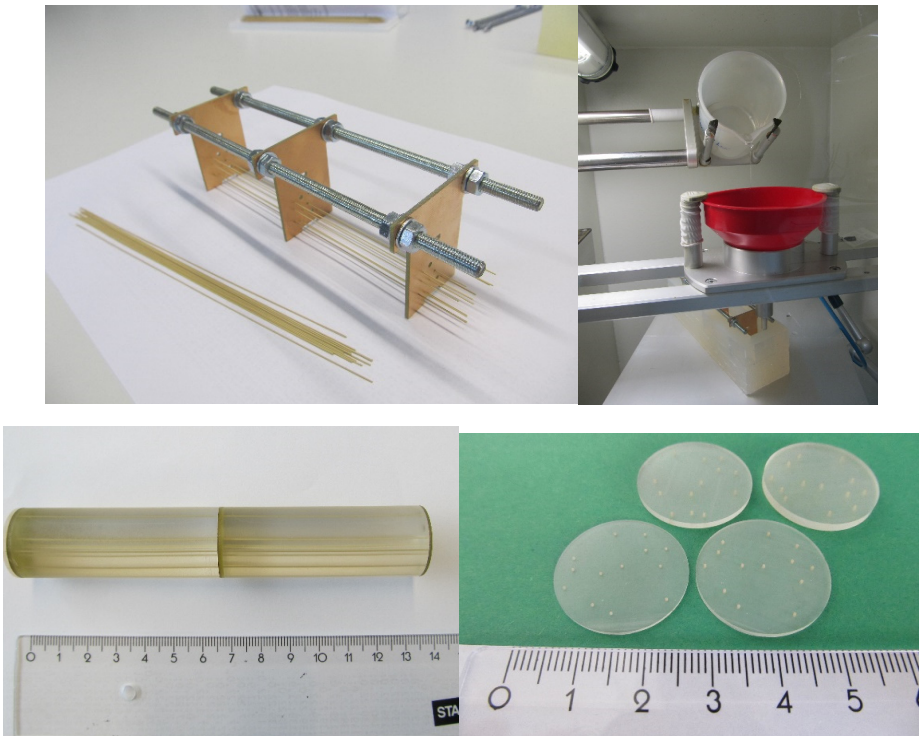

Figure 11: Fibre composite disc production: top left putting the sintered piezo fibres into the mask, top right: filling the mould with epoxy as substrate, bottom left: cured and mround milled rod, bottom right: sawed to four different thicknesses piezo discs

Then, the discs got a front common ground electrode by sputtering and individual connections per fibre. Then the discs weres poled with approx. 2kV/mm.

3.2 Transducer design and built up process

The prototypes are built piezofibre from the piezofibre discs glueing them to a TMM 26.75mm diameter front matchin plate of 470µm thickness Rogers TMM4 disc, a high-frequency aluminium oxid based PCB material. The glueding was done with conductive silver-glue also providing the common ground connection, see Figure 12 top right.

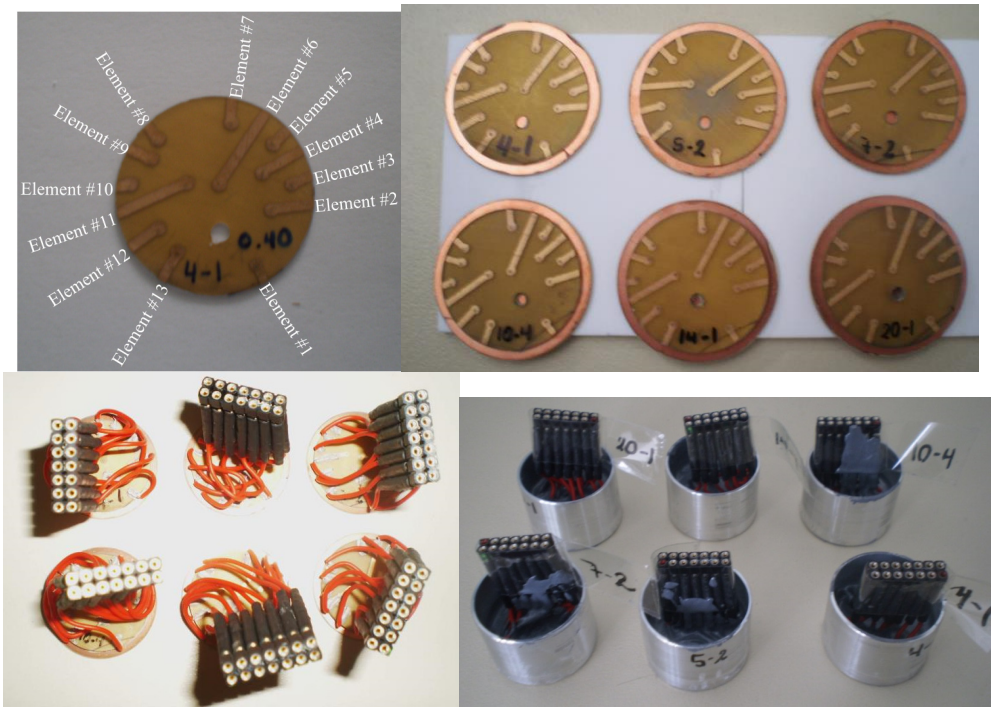

Figure 12: Schematic of the whole build-up process for the six transducer prototypes.

3.3 PCB design

A Flexprint design was choosen as PCB base for electrical connectivity for the transducers (not shown in the prototypes).

The design has many holes acting as pinholes for X-Y position accuracy (~0.05mm) and for later underfilling and getting rid of air. The backsite has substrate defined pads of 400µm diameter. The layout and final product are shown in Figure 13.

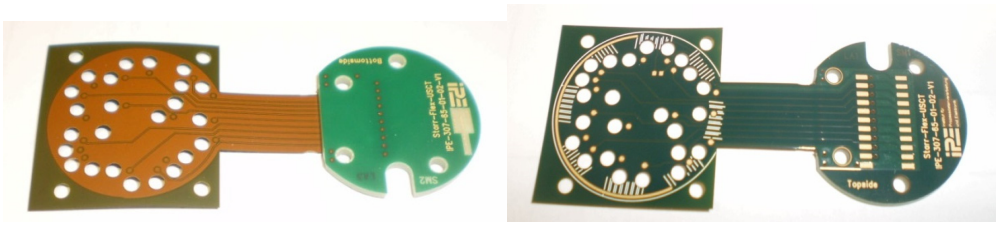

Figure 13: Flexprint PCB layout top side (left) and flex-print PCB backside (right).

3.4 Backing

3.4.1 Tungsten + PU backing

As backing some improved formula of the 3D USCT II baking was used: 1g VOSSFlex 2k Polyurethane filled with 2.5g Tungesten with 10µm particle size [10]. This resulted in a strongly attenuating composite of PU and tungsten powder which is also a well matching with an acoustic impedance values of approx. 11 MRayl. The mixing process was supported by 1% defoamer, the mixture was extensively, manually (~30min) degassed in vacuum chamber going to ca 50mbar.

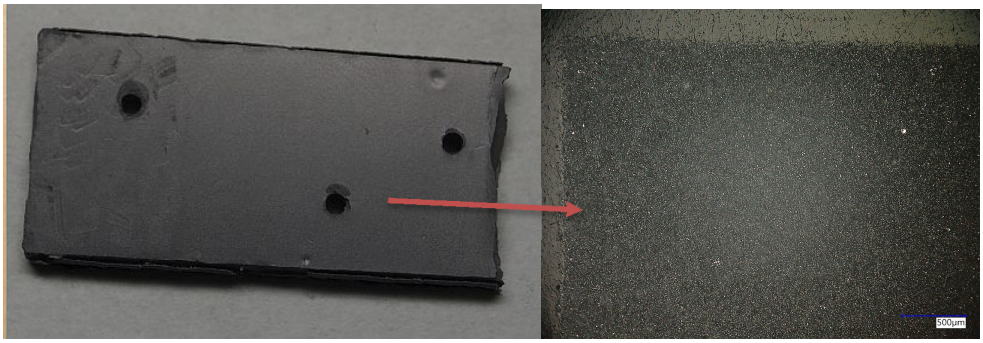

Figure 14: (left) PU-tungsten composite material, (right) its lower part under the microscope. Degassing is effective; no major air inclusions are visible (left).

3.5 Gluing and electrical connectivity

1K Heraeus PC3000 silver glue is used to electrical connect the individual elements. Curing is achieved with 100C° for half an hour on n temperature regulated heating plate.

A sieve printing mask test of 400µm, 500µm, 600µm dots diameter sizes was developed to analyze and optimize the individual element connect.

3.6 Matching and glueing

3.6.1 TMM4

The acoustic impedance of Rogers TMM4 an aluminum oxide composite with of 6.4 MRayl acoustic impedance is near optimal for a single-layer matching between PZT and water. TMM4 is a very stiff, mechanical mil-and drillable material and exhibits low water absorption. Besides being a strong electrical insulator, thermal conductivity of TMM4 is quite high. This is helpful for correct water temperature measurements, as the USCT temperature sen-

sors are situated behind the TMM4 plate. Final waterproofing will be achieved with a thin layer of parylene.

4 Evaluations and results

4.1 Electrical Characterization

The sputtered piezofibre discs were analyzed with a fast electrical characterization in phase (see Fig. 15) and impedance between 500 kHz and 6 MHz. The HP 4194 phase analysator was calibrated before usage and every element of the 13 elements was measured of the selected six piezofibre discs shown in Fig.16.

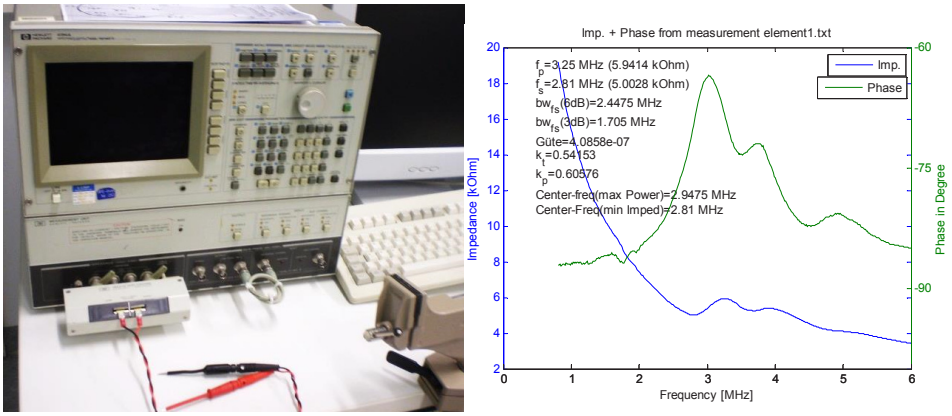

Figure 15: Impedance spectroscop used to characterize the build up prototypes (left). Example impedance and phase measurement graph of one element (right).

As result of the electrical characterization the thicknesses 400, 550, and 750µm were considered for further analysis; thicker disc thickness were not analyzed further due to poor performance and low sound pressure.

Thickness of disc (in µm)	Center freq. (in MHz @max. Power, mean/std.)	BW (max. Power@ 3dB/6dB)	Phase (in degree@max. Power)	Kt (mean/std.)	Working (kt >0.1)
400	3.01 (0.24)	1.69 / 2.34	-69.98°	0.56 (0.17)	**11/13**
550	2.54 (0.07)	1.57 / 1.99	-72.24	0.84 (0.06)	**12/13**
750	2.06 (0.11)	1.23 / 1.34	-74.53	0.90 (0.01)	**13/13**
1050	3.56 (1.29)	0.17 / 0.17	-85.08	0.91 (0.03)	**4/13**
1450	3.34 (0.07)	1.62 / 2.54	-85.22	0.11 (0.24)	**1/13**
2050	2.53 (0.04)	1.25 / 1.73	-85.30	0.00 (0.00)	**1/13**

Figure 16: Table of the results of the impedance phase measurement of the analyzed 6 piezofibre discs.

4.2 Acoustical measurements

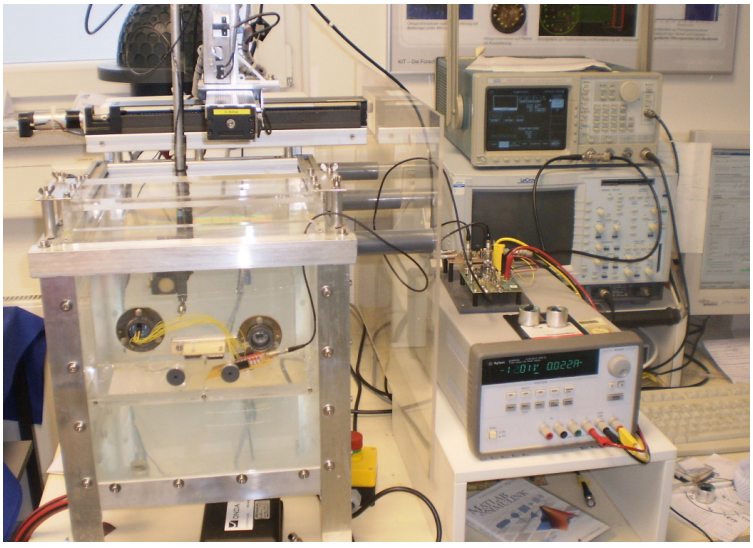

Figure 17: Left: measurement container (30 x 30 x 50 cm), top: 3-movement axis with stepper-motors and mounted hydrophone, bottom left: sockets for transducers, right: AWG, HV amplifier, DAQ, and control PC.

Ultrasound characteristics were evaluated quantitatively with a hydrophone in a 3-axis water tank for selected sample transducers [8, 9].

The measurement tank is a self-built system. The excitation voltage used was +-/100Vpp for a frequency sweep with chirps of 0.5MHz to 5.5MHz in 250kHz steps. A calibrated Onda HNC-400 hydrophone (up to 10MHz) with a 20dB pre-Amplifier was used. In the measuremenet procedure 16x averaging of the measurement was used to achieve a 4x SNR gain. The measured signal digitization length was 400µs with as sampling rate of 20MHz. Overall measurement time per prototype was several hours. The resulting performance for the thicknesses 400, 550, and 750µm can be seen in Fig. 18.

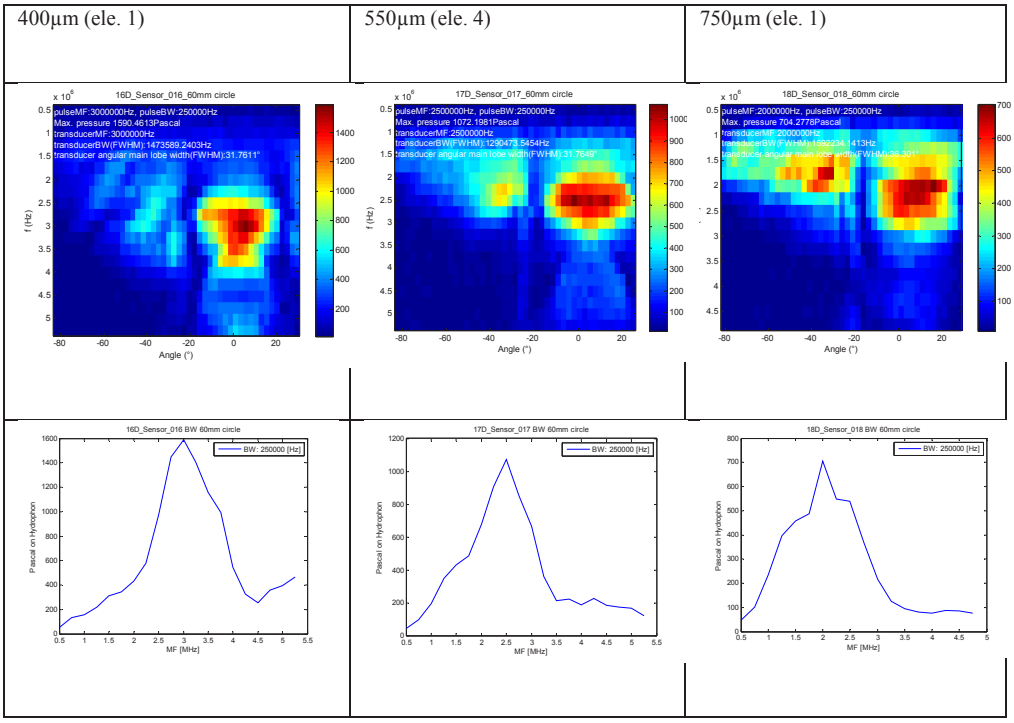

Figure 18: Acoustical characterization of transducer prototypes of varying dic thickness, top row: sound pressure over angle and frequency, bottom row frequency characteristic.

5 Discussion and conclusion

Funtionality and reliability of the piezofibre discs as analyzed with a phase impedance analysator and the reliability of >92% was encouraging. Then six prototypes of varying dis were build up to select the preferred center frequency and bandwidth; the 750µm thickness was selected. The developed PU-tungsten composite backing material led to a significant

increase in BW through improved acoustic matching to the rear of the transducer in co-maprision to the original 3D USCT transducer design. This it can be seen in the acoustical measurements in fig. 18. Also, future by USCT utilized imaging techniques like paraxial wave inversion approaches benefit greatly from lower frequency <1MHz (down to approx. 0.5MHz) now available due to the extended bandwidth.

Analysis of the integration and connectivity process of the TMM4 ceramic matchin layer is ongoing. The curently semi-automatized process leads still to variations and in result to the failure of a signifcant portion of the transducer elements; especially in the glueing and filling step. This is currently under intensive investigation with further test prototypes. Final step to adapt and integrate the electronic front-end board (pre-amp and MUX) and the housing are the next steps in finalizing the production process.

References

[1] [Online]. Available: http://www.wcrf.org/int/cancer-facts-figures/data-specific-cancers/breast-cancer-statistics.

[2] [Online]. Available: http://www.who.int/cancer/detection/breastcancer/en/index1.html..

[3] James S Michaelson et al., „“Predicting the survival of patients with breast carcinoma causing tumor size,“ Cancer, 2002.

[4] Ruiter et al., „Realization of an optimized 3D USCT,“ SPIE 7968, Medical Imaging 2011: Ultrasonic Imaging, Tomography, and Therapy,, 2011.

[5] T. H. M. Z. C. K. N. R. H. Gemmeke, „3D ultrasound computer tomography. hardware setup, reconstruction methods and first clinical results.“.Nuclear Instruments and Methods in Physics Research Section A: Accelerators, Spectrometers, Detectors and Associated Equipment.

[6] Gemmeke et al., „An improved 3D Ultrasound Computer Tomography system”. IEEE International Ultrasonics Symposium., 2014.

[7] G. Göbel, „Entwicklung von Ultraschallsensorarrays mit miniaturisierten Komponenten,“ Diploma, KIT, 2002.

[8] M. Zapf, „Simulation eines Ultraschalltomographen im k-space,“ in Master thesis for Hochschule Karlsruhe (University of Applied Science), Karlsruhe, 2010.

[9] L. Petzold, „Aufbau eines Messplatzes zur Ermittlung der Schallfeldcharakteristik,“ Master thesis, KIT, 2006.

[10] G. Shah, „Auto-Calibration of Ultrasound Transducer Characterization Setup,“ Master thesis, KIT, 2015.

[11] P. Pfistner, „Composite-based ultrasound transducers for a 3D-Ultrasound computer tomograph,“ Master thesis, KIT, 2017.

[12] B. Kohout, „Finite Elemente Simulation von Ultraschallwandlersystemen für die Ultraschall Computertomographie,“ KIT, Diploma , 2010.

[13] G. S. M.Zapf, „Aperture optimization for 3D ultrasound computer," IEEE UFFC Symp., 2007.

[14] N. R. H. Gemmeke, „3D ultrasound computer tomography for medical," Nuclear Instruments and Methods in Physics Research Section A: Accelerators, Spectrometers, Detectors and Associated Equipment, 2007.

[15] K. Hohlfeld, S. Gebhardt, A. Schönecker, A. Michaelis: „PZT components derived from polysulphone spinning process". In: Advances in Applied Ceramics 2015; 114(4), 231-237.

[16] M. Zapf, K. Hohlfeld, G. Shah, S. Gebhardt, H. Gemmeke, A. Michaelis, N. V. Ruiter: „Evaluation of piezo composite based omnidirectional single fibre transducers for 3D USCT". In: Proc. IEEE Int. Ultrasonics Symp., October 21-24, 2015, Taipei (Taiwan).